CP Algorithm Theoretical Basis Document

NMSC/SCI/ATBD/CP, Issue 1, rev.4

26 December 2012

REPORT SIGNATURE TABLE

Function	Name	Signature	Date
Prepared by	Yong-Sang Choi, Heaje Cho		26 December 2012
Reviewed by	Yong-Sang Choi		26 December 2012
Authorised by	NMSC		26 December 2012

DOCUMENT CHANGE RECORD

Version	Date	Pages	Changes
Version 4	2012.12.26	-	-Nothing has changed for contents besides ATBD form.

Table of contents

List of Tables

List of Figures

List of Acronyms

COMS	Communication, Ocean, and Meteorological Satellite
MTSAT	Multi-functional Transport Satellite
JAMI	Japanese Advanced Meteorological Imager
ISCCP	International Satellite Cloud Climatology Project
FOV	Field of view
MODIS	Moderate Resolution Imaging Spectroradiometer
CP	Cloud Phase
SBDART	Santa Barbara DISORT Atmospheric Radiative Transfer

1. Overview

Cloud phase (CP) is a product that plays a decisive role in determining the radiative properties of clouds before other cloud information is retrieved. Cloud Phase is key information to classify climate monitoring and semi-transparent clouds or thin cirrus at EUMETSAT Satellite Application Facilities (SAF). It is also used to determine the growth process of strong convective clouds(Key and Intrieri 2000).

2. Background and purpose

In order to retrieve the cloud phase, Strabala et al. (1994) suggested CP retrieval using 8.7, 10.8, and 12.0㎛ channels using absorptance differences depending on the wavelength of ice phase and water phase clouds. This method is widely used in MODIS CP algorithms.

However, COMS meteorological imager do not have the most important 8.7㎛ channel. So, it was a difficult to use the method by Strabala et al.(1994). Tests using this channels determines the classification of ice phase clouds (Baum et al. 2000). The COMS CP algorithm is an improved algorithm for the classification of ice phase clouds using water vapor absorption channels (Choi et al. 2007).

3. Algorithm

3.1. Theoretical background and basis

The CP algorithm divides the cloud into water, ice, mixed, and uncertain phases. The CP algorithm used the 10.8㎛ and 12.0㎛ atmospheric window region based on the prototype for the MODIS cloud phase algorithm. In order to improve the accuracy of ice phase retrieval in high level clouds, we added the 6.75㎛ water vapor absorption channel.

The CP algorithm is composed of a combination of test methods using the static threshold value. Indistinguishable pixels in each test process are classified as ‘uncertain’. Streamer (e.q. Radiative Transfer Model) was used to decide the threshold value of each test. It used 15 day MODIS observation data. This CP algorithm fundamentally uses the absorption difference between water and ice particles of clouds in infrared channels. Fig. 1 is shows the refractive index of ice and water phases for wavelength groups, which calculates the absorptance. The absorptance of cloud phase of water and ice phases is different. The larger absorptance, the smaller the emitted radiance. Therefore, radiances

of 6.7 ㎛, 10.8 ㎛, 12.0 ㎛ have different values depending on the phase of the cloud particle. This is the principle behind dual spectrum IR tests.

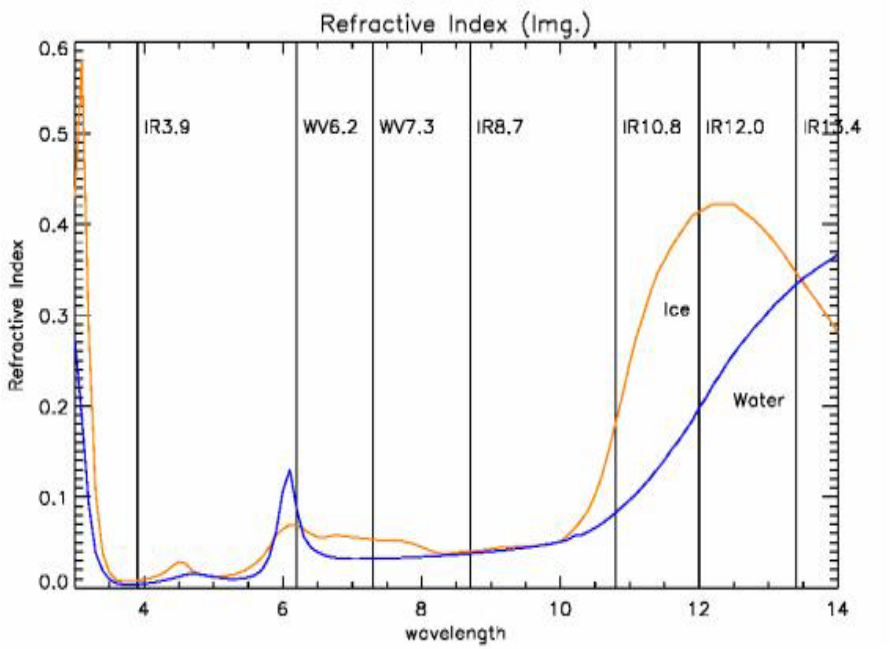

Fig. 1. Imaginary refractive indices of ice and water

3.2. Retrieval method

3.2.1. Look-up table retrieval method

The CP module developed for the prototype is based on the MODIS algorithm. However, ice phase retrieval accuracy is expected to be lower compared with MODIS. This is because the 8.7㎛ channel data plays an important role in retrieving cloud phase, but is not observed by COMS satellites. Therefore, this CP module complements in the absence of 8.7㎛ channel and focuses on the method to improve the accuracy of ice phase retrieval. The possibility is the utilization of the 6.7㎛ water vapor absorption channel (Choi et al. 2007 IJRS). The retrieval of cloud phase using 3.7㎛ has been studied for NOAA/AVHRR sensors unable to use 8.7㎛, but this channel has to consider many factors such as surface properties, cloud top temperature, land surface temperature, and sun incident angle in the retrieval time (Key and Intrieri 2000). The 6.7㎛ channel has been used mainly to detect high

level clouds through features of water vapor in the troposphere. This CP module is used for classifying high level ice phase clouds with the 6.7㎛ channel, which is based on the research of Choi et al. (2007).

3.3. Retrieval process

Cloud phase is retrieved through three threshold tests in Fig 2. The first is a test of simple threshold value using the brightness temperature of the 10.8㎛ channel. The second test uses the difference of brightness temperatures in the 10.8㎛ and 12.0㎛ channels. The final test is used mainly for the detection of ice phase using the brightness temperature of the 6.7㎛ channel.

The three tests are first run simultaneously to determine ice phase. If the pixels are determined to be ice phase, it goes on to the classification step of mixed phase using the BT 10.8 and BT 6.7 tests. If the pixels are determined to be mixed phase, it goes on to the water phase. If this step is determined to be water phase, it is divided into uncertain phase.

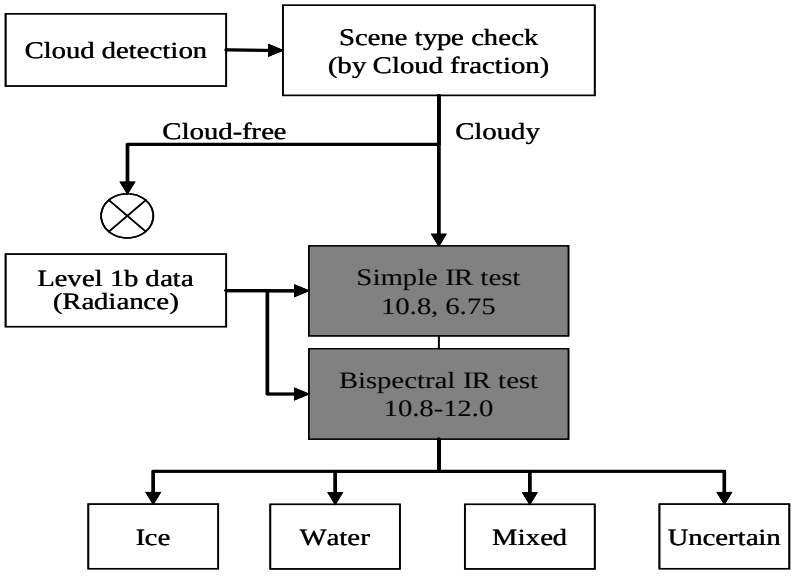

Fig. 2. Flowchart of the methodology for the retrieval of CP.

3.3.1. Threshold value test

This CP algorithm consists of two tests of simple IR (BT10.8, BT6.7), and three threshold value tests of IR channel difference (BTD10.8-12.0). The threshold value for each test was decided through simulation results by Radiative Transfer Model (RTM) and validation of MODIS products. The reason it is used as for validation MODIS product is because this CP algorithm used the method of Strabala et al. (1994) based on the MODIS prototype. The Radiative Transfer Model (RTM) for the decision of threshold value used the Streamer model (Key and Schweiger 1998).

Atmospheric vertical distribution (temperature, humidity, ozone) need to simulation used the standard distribution of polar region, mid-latitude summer and winter region, and the tropic region accumulated by Ellingson et al.(1991). This section shows the simulated results for a standard atmospheric profile (land surface temperature 293K, surface albedo 0.1) of mid-latitude summer (Fig. 3). High level ice phase clouds are located at a height of 300hPa. Low level water phase clouds are assumed to be located at a height of 500 hPa. At 500 hPa, water phase clouds must be the highest that have a standard atmospheric profile in the mid-latitudes.

The scattering of cloud particles assumed that it had a spherical surface regardless of the particle composition. It was calculated using Mie scattering. The particle density of clouds in water phase is 0.2 gm^{-3}, the particle density of clouds in ice phase is 0.02 gm^{-3}. This is shown in the following:

```
; Streamer input file to calculate COMS CP thresholds

OPTIONS
.FALSE.          ; Compute fluxes (or radiances)?          (FLUXES)
.FALSE.          ; Include thermal emission in 3.7um band? (IR106)
.FALSE.          ; Compute cloud forcing?                  (CLDFRC)
4 12             ; Number of streams, short and long       (NSTR*)
24               ; Number of Legendre coeff.               (NCOEF)
.FALSE.          ; Include gaeous absorption?              (GASABS)
.FALSE.          ; Include Rayleigh scatter (shortwave)?   (RAYISHRT)
2                ; Surface albedo control                  (ALBTYPE)
4                ; Surface emissivity control              (EMISSTYPE)
2 .FALSE.        ; Std prof; extend input profile to 100 km? (STDPROF,SPACE)
```

```
1 1                    ; Aerosol model and profile              (AERMOD,ERVERT)
1 1 3 1 1 3 4    ; Units                (IZD,ITD,IWV,IO3,ICTOP,ICTHK,IWAVE)
1                      ; Output levels control                  (OUTLEVS)
.FALSE.              ; Descriptive output desired?              (DESCRIP)
comscp.des
.TRUE.               ; User-customized output?                  (USEROUT)
str_water_nogas.out
coms.wts
.FALSE.          ; Read cloud optical properties?           (USERCLOUD)
                  ; cloud filename (USERCLOUD=.TRUE.)         (CLOUDFILE)
                  ; BRDF filename (ALBTYPE=7)                (BRDFILE)

CPRINT channel, cldre1(1), cldtau(1), \
          sattb(1,1), sattb(2,1), sattb(3,1), \
          sattb(1,2), sattb(2,2), sattb(3,2)

SETDATA
No name
1999 6 21 12.0 0 0 0
3 0.5 0.87 1.0 2 10.0 180.0
3
0.1 1 1 1.0
-999. 0.99
1 1 1.0 -999 500 999 5. 1 0 10. 0.02 999 999 999
0
2 2 2 2 2 2 0 1.0 1.0 1.0 1.0 1.0 1.0

REPLACE channel=[2,3,4,5],cldre1(1)=[5,8,16,32],cldtau(1)=[0,0.2,0.5,1,2,3,5,10]
```

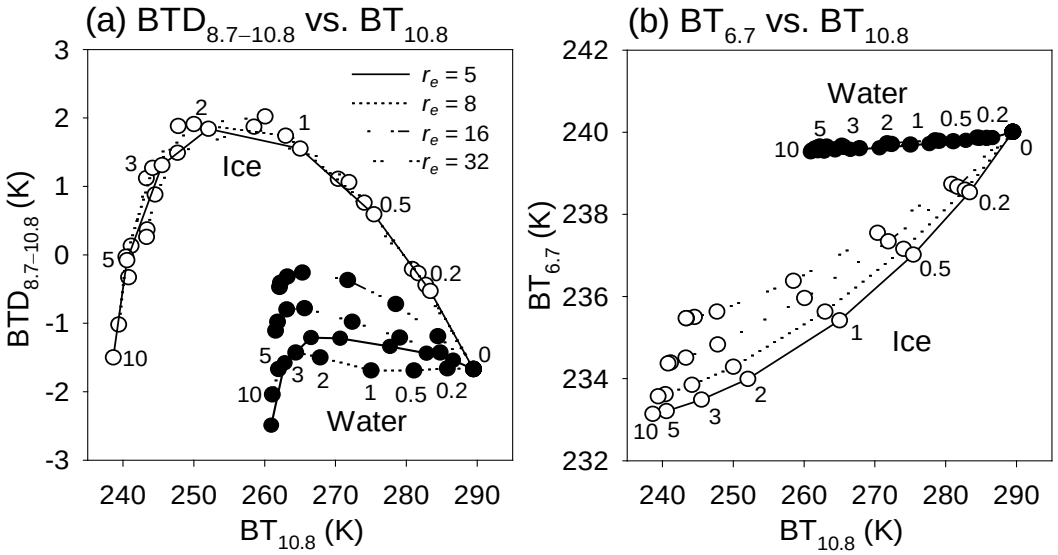

Fig. 3. The results of RT model simulation for (a) BT10.8 versus BTD8.7-10.8, (b) BT10.8 versus BT6.7 for clouds composed of water droplets (filled circle) and ice crystals (open circle). The numbers indicate cloud optical thickness. re stands for effective particle radius.

The most important threshold value test of the CP algorithm is a simple IR test using a brightness temperature of 10.8㎛. The ice phase of BT 10.8 is from 240K to 290K in Fig. 3. Water phase has a value from 260K to 290K. The standard atmospheric profile of mid-latitude winter or polar region has a lower value than these. Brightness temperature generally classifies into ice phase below minus 40 ℃, mixed phase between -40 ℃ and -10 ℃, and water phase above -10 ℃. This criteria is statistically decided using aircraft observation results and simulated results of RTM in the America (Baum et al. 2000). The IR channel difference (BTD 8.7-10.8) tests of the MODIS CP algorithm are a necessary test to classify ice phase (Baum et al. 2000). Ice phase can have the value of BTD 8.7-10.8 above 0, but water phase cannot. In this CP algorithm, the test uses brightness temperature of 6.75㎛ in an alternative test of IR channel difference (BTD 8.7-10.8) (Fig 3).

Ice phase can have a value of BT 6.7 below 239K, but water phase clouds cannot. Therefore, pixels with a BT 6.7 value below a certain threshold value can classified as ice phase. The threshold value of the IR channel difference test (BTD 10.8-12.0) is also used for classifying of ice phase. The change of BTD 10.8-12.0 value of ice phase and water phase in the same condition looked through RTM simulation. The BTD 10.8-12.0 for ice phase value is above 4.5K or water phase is not in Fig. 4.

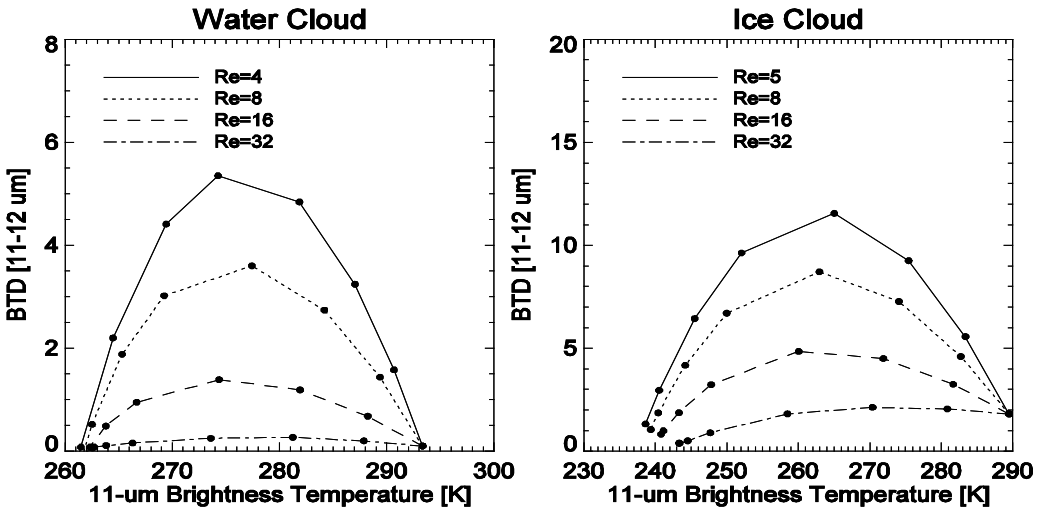

Fig. 4. BTD10.8-12.0 distribution with respect to BT10.8 for water (a) and ice cloud (b) that have a variety of effective particle radius(4 or 5, 8, 16, 32) and cloud optical depth(0.1, 0.2, 0.5, 1, 2, 3, 5, 10).

The substantive relationship with BT 6.7, BT 10.8 and cloud phase investigated using MODIS cloud phase data. MODIS data is used to collocat data for mid-latitude and the tropic region between March 1-16 2000. Fig. 5 shows the scatter plots of BT 6.7 and BT 10.8 corresponding to MODIS cloud phase and data. Pixels classified as ice phase in MODIS have a BT 10.8 smaller than 238K and a BT 6.7 smaller than 250K. In fact, BT 10.8 of 238K is the threshold value of the ice phase in the MODIS algorithm. Values between 234K and 250K in BT 6.7 can have the pixels classified simultaneously as ice phase, water phase and mixed phase. This is in accord with the results of the previously simulated BT 6.7. Therefore, BT 6.7 brightness temperatures under 230K can distinguish ice phase, between 234-250K is mixed phase, and more than 250K is water phase.

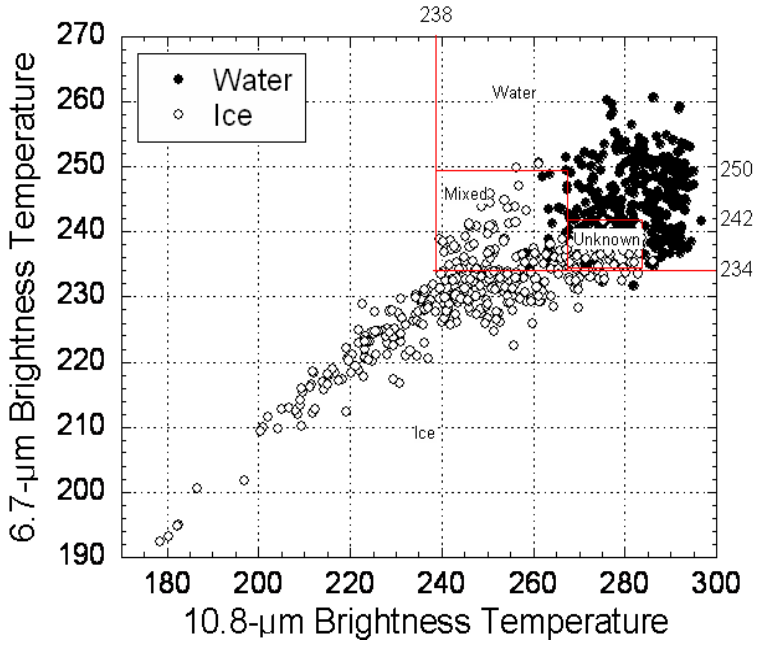

Fig. 5. Scatter plots of MODIS cloud phase product.

3.3.2. Multi-layer clouds

This module used Steamer of the Radiative transfer model to judge whether it is valid for multi-layer clouds. The Model assumed that the cloud exists in two layers. This algorithm assumes that high level ice phase clouds have an effective particle radius of 30㎛ and are located at a height of 300hPa. Low level water clouds have an effective particle radius of 10㎛ and are located at a height of 700hPa.

Effective particle radius value is used for retrieval process of ISCCP data. The particle density of water phase clouds is 0.2gm^{-3}, and the particle density of ice phase is 0.07 gm^{-3}. The variation of brightness temperature is calculated with cloud optical thickness as 0.1, 0.5, 1, 2, 3, 4, 5, 10, and 20 in water phase clouds, and 0.1, 0.5, 1, 2, 3, 4, and 5 in ice phase clouds.

Fig. 6 shows the change of BT 10.8 and BTD 10.8-12.0 that two clouds with various heights can represent with each various optical thickness. High level ice phase clouds and low level water phase clouds have very different values when in a simple layer. The difference is that high level ice phase clouds get optically larger and thicker. On the other hand, if high level ice phase clouds are optically a very thin, there is no difference with low level water clouds.

If two layers exist, low level ice phase clouds with the same optical thickness have a low optical

value as it gets thicker. If the optical thickness of high level ice phase clouds is more than 5, its decrement is small. Optical thickness of high level ice phase clouds is the deciding factor of BT 10.8 value. If thin high level ice phase clouds over low level water phase clouds exist, BT 10.8 will decrease sharply. The setting of threshold value both minus 40℃ and minus 10℃ of the simple IR test through this analysis could know the significance for high level cloud when multi-layer clouds existed. Especially BT 10.8 is classified as ice phase when it is lower than minus 40. This means cloud phase for existing cloud at the highest level. In the case of BTD 10.8-12.0, the effect of multi-layer cloud is not so big (Fig. 6b).

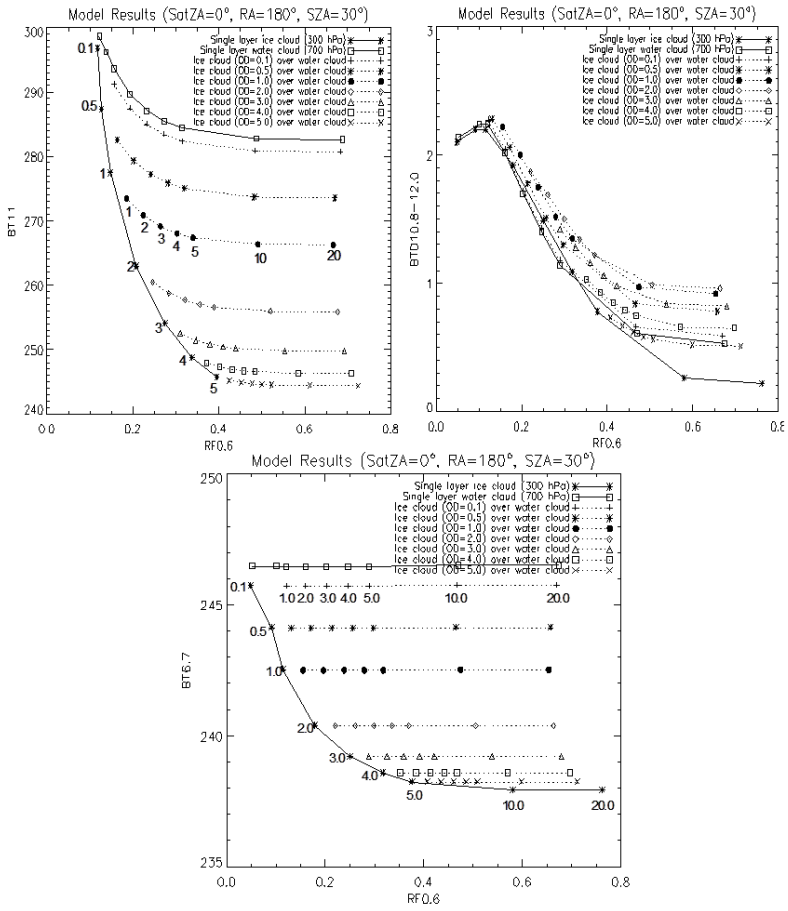

Fig. 6. Calculations of 0.6㎛ reflectance and BTD10.8-12.0 for a single-layer water cloud, a sing-layer ice cloud, and ice cloud overlapping a water cloud. The clouds are shown as a function of visible optical depth which ranges are from 1.0 to 20.0. SatZA, RA and SZA denote satellite zenith angle, relative azimuth angle between the sun and satellite, solar zenith angle, respectively.

We simulated for simple IR test module of 6.7㎛ using RTM. High level ice phase and low level water phase existed at the same time, which matched the method performed for the simple IR channel test module of 10.8㎛ (Fig. 6c). BT 6.7 seems uniformly to be keeping irrespective of the existence of low level clouds, and this value can be known depending on the optical thickness of high level clouds (Fig. 6). If optical thickness is a smaller cloud, it have a high brightness temperature, because it is less absorbed when the radiation emitted in lower atmosphere of high level cloud pass through clouds. On the contrary, optical thick clouds in high level have a low brightness temperature as the radiation emitted in the top of cloud reach on satellite.

3.3.3. Determination of threshold value

Cloud phase determined through the above steps describes the threshold value. The cloud phase algorithm is retrieved through three tests (Table 1). BT 10.8 and BTD 10.8-12.0 tests will be applied the concept of MODIS algorithm. BT 6.7 test is used to mixing for BT 10.8 or BTD 10.8-12.0 test and each cloud phase determination step.

First, the three tests are used at the same time to determine ice phase. If the pixels are distinguished as ice phase, it moves on to discriminate mixed phase using the BT 10.8 and BT 6.7 tests. If the pixels are determined to be mixed phase, it moves on to the water phase step. if this step is distinguished as water phase, it is classified as uncertain phase.

Table 1. The criteria for determining cloud phase

Required tests for cloud phase		
Ice	Mixed	Water
BT10.8 < 238 K or BTD10.8−12.0 ≥ 4.5 K or BT6.7 < 234 K	For no ice 238 K ≤ BT10.8 < 268 K or 234 K ≤ BT6.7 < 250 K	For no ice/mixed BT10.8 ≥ 285 K or BT6.7 ≥ 250 K

3.3.4. QC flag

QC flag for cloud phase are suggested in Table 2. When cloud phase has ice phase, mixed phase, and water phase, it gives the flag considering brightness temperature observed in several channels. For ice phase, it gives the flag up to 32-129. For water phase, it gives the flag of 8 and 16. In the case of

water phase, it gives the flag of 2 or 4.

Table 3. QC flag for CP

CLA - CP		
bit	**Bit Interpretation**	**Field Description**
8~2 (Pixel weights in terms of the cone zenith angle.) **1**(reserved) **unavail => 0**	128 64 32 16 8 4 2	BT10.8 test for ice phase BT(10.8-12.0) test for ice phase BT6.8 test for ice phase BT10.8 test for mixed phase BT6.7 test for mixed phase BT10.8 test for water phase BT6.7 test for water phase

3.4. Validation

3.4.1. Validation method

Validation of cloud phase was executed by two methods for real-time validation applied by CMDPS and self-validation of developer, respectively.

3.4.1.1. pre-processing for validation-simplified ISCCP cloud detection

Hourly Full-disk provided from Japanese Advanced Meteorological Imager (JAMI) sensors on board Multi-functional Transport Satellite (MTSAT) was used as input data for calibrated radiance and brightness temperature of a simulated COMS images. The central wavelength of 5 channel from JAMI are located at 0.725㎛ (VIS), 10.8㎛ (IR1), 12.0㎛ (IR2), 6.75㎛ (IR3), and 3.75 ㎛ (IR4). Pre-processing distinguishes clear pixels between clouds and clear in order to validate cloud information.

현업에서는 CMDPS 알고리즘에서 구름탐지 알고리즘이 이 역할을 담당하나, 본 알고리즘의 검증은 간소화된 International Satellite Cloud Climatology Project(ISCCP) 구름탐지 기법을 활용하였다.

In the operation, the cloud detection algorithm played the role of the CMDPS algorithm, but this algorithm validation utilized simplified cloud detection techniques (Rossow and Garder 1993a) of the International Satellite Cloud Climatology Project (ISCCP). For cloud detection, ISCCP uses the spectral test of VIS and IR channels as follows:

Clear: $(BT_{IR1}^{clr}-BT_{IR1})\leq$IRTHR and $(L_{VIS}-L_{VIS}^{clr})\leq$VISTHR

Cloudy: $(BT_{IR1}^{clr}-BT_{IR1})>$IRTHR or $(L_{VIS}-L_{VIS}^{clr})>$VISTHR (1)

BT_{IR1}^{clr}, BT_{IR1}, L_{VIS}, and L_{VIS}^{clr} are IR1 brightness Temperature in all sky, IR1 brightness temperature in clear sky, radiance of VIS in all sky, and radiance of VIS in clear sky, respectively. L_{VIS} is the adjusted radiance by the percent ratio, which is the same as in the ISCCP algorithm. IRTHR of threshold value is 12.0 K, VISTHR is 6.0% for the land, and 3.0 for the ocean. The availability of cloud detection will have to be decided mainly by the accuracy of the clear sky radiance (Rossow and Garder 1993b). In this validation, BT_{IR1}^{clr}(L_{VIS}^{clr}) set the maximum (minimum) value for each UTC in the month of August, 2006. VISTHR is the same as the value of ISCCP, because it is highly calculated brightness temperature of IR clear sky. IRTHR is 6K higher for land, and 1K higher for oceans than the values suggested by Rossow and Garder (1993a). Therefore, the selection of cloud pixels is stricter than the ISCCP algorithm. We use IR conditions of equation (1) during nighttime.

The detected cloud amount by the above method account for the average CA for August, 2006, which are about 57.3 % in JAMI Field Of View (FOV). This value is comparable with estimated results of other global CA climate data. Rossow et al. (1993) estimated 62.7% in ISCCP C2 (1984-1988), 61.2% in gridded surface weather station reports (SOBS) (1971-1981), 61.4% in METEOR (1976-1988), and 51.8% in Nimbus-7 (1980-1984).

One point of notice is higher than JAMI cloud amount. The MODIS cloud amount has an average of 77.6%. It has 18 bands from MODIS in narrower Field of View (FOV), because it detects various shaped clouds, including thin cirrus. Therefore, the results of cloud detection by this method will contain a considerable uncertainty as compared with reality. . It is obvious that have cloud information product or uncertainty using above method is obvious.

3.4.1.2. Explanation of validation method (developer validation)

Validation is performed for JAMI Full-disk images in August, 2006. This period was chosen to analyze a limited calculation space, but Field of view (FOV) of this period includes all situations; surface, cloud type, vertical distribution of atmospheric gas, observation and sun zenith angle that affect on geostationary satellite detection. In addition, during this period, typhoons such as Saomi and Bopha reached the Korean Peninsula and Japan. Since the main purpose of COMS utilization is to

predict heavy weather, this validation period is optimal for examining the performance capacity of the algorithm.

In this validation, cloud products of two type were improved the current version in comparison/validation with “base product” retrieved by traditional algorithm and the “final product“ of the current version algorithm(Choi et al. 2007) with independently developed by Prof. Chang-Hoi Ho team in Seoul National University. Basic cloud phase is retrieved using the IR1 and IR2 channels, and final cloud phase uses the IR1, IR2, and IR3 channels. Compared with basic cloud phase and final cloud product, it is possible to see the role of IR cloud phase tests introduced by Choi et al. (2007). The designations of each product used in this validation are summarized in Table 3.

Table 3. Definitions of terms used in this analysis.

Term	Unit	Definition
Base CP	unitless	Cloud phase is determined by BT_{IR1} and $BT_{IR1}-BT_{IR2}$ tests
Final CP	unitless	Cloud phase is determined by BT_{IR1}, $BT_{IR1}-BT_{IR2}$, and BT_{IR3} tests in table 1.

As pointed out above, the defined base, final, and MODIS products compared as four procedures. All of four results correct the algorithm in optimal conditions, and provides useful data to comprehend the weak points.

(1) Scene analysis

Scene analysis is the first part of this validation. Scene analysis means a comparison between radiance and product. It can roughly review total reliability of the product.

(2) Comparison with climate data

Comparison with climate data identifies whether the product is reliable as climate data. Also, product data can determine bias. Long term data must be obtained, but this validation was limited to August, 2006. Climate data can figure out the cause of bias for retrieval value divided and compare it to a variety of conditions. For example, It compares MODIS climate data for day, night, water phase clouds, ice phase clouds, southern hemisphere, northern hemisphere, the Antarctica, the tropic region, and the mid-latitude region.

(3) Time-series comparison

Time-series comparison compares validation ancillary data and diurnal variation during a validation period for a region of interest. The region selected are divided between the land, ocean, desert, snow/ice and various surface conditions, low, middle, and high latitudes. Region of interest selected in this validation are 9 region; Seoul, the Hwabuk plain in China, the Gobi desert, the Tibetan plateau, the South China Sea, the East Pacific, the Bering Sea, and the Antarctica.

(4) pixel comparison

Finally, we examine the error range in comparison with ancillary data into pixel units for cloud information product. In this validation, MODI06 collocation 5 cloud data was used as ancillary data. The difference between cloud phase image pixels of MTSAT and MODIS can cause uncertainty of comparison results in this pixels. Choi et al. (2007), compared the retrieved results performing as input MODIS brightness temperature and the retrieved results of MODIS cloud phase. In this case of the pixels of our product exactly corresponded with MODIS product.

3.4.2. Validation data

(1) CMDPS validation

Cloud phase was validated based on MODIS satellite data. The data is divided into Terra and Aqua satellites. The date used is from November 1 to 5.

(2) Developer validation

JMAI radiance and the spatial resolution of observation angle used for validation is 4km.

Full-disk image is similar to the location of COMS including East Asia and the Western Pacific, Australia, and the Antarctica part (80.5°S-80.5°N, 60.4°E-139.4°W). We used MODIS cloud data to compare with JAMI image product. This data includes 5km resolution cloud phase for nadir (Platnick et al. 2003). This improves on the previous version in collection 5 data, which can be found in Baum et al. (2005), King et al. (2006), Yang et al. (2007). MODIS granules (5-min data) were collocated for the Pacific Northwest (10°-30°N, 113°-149°E) from 5-11 August 2006. The recent MOD06 cloud phase is retrieved using Bispectral IR and Shortwave IR tests. The Bispectral IR test uses 8.5㎛ and 11㎛ bands(Menzel et al. 2006). This method is a simplification of the trispectral IR test using 8.5, 11, and 12㎛ introduced by Strabala et al. (1994)

Shortwave IR 시험은 가시광, 근적외, 적외 밴드를 혼합하여 쓰는 방법인데 구름광학두께

산출 모듈의 일부분이기도 하다

Shortwave IR test uses to mixing visible, SWIR, IR bands. It is part of module of cloud optical thickness retrieval (King et al. 2006). Reliability is retrieved high estimation because Shortwave IR tests use more channel information. This method is only possible during the daytime, but it is difficult to use the MTSAT-1R channel. Therefore, this validation used MODIS cloud phase retrieved from the Bispectral IR test.

MODIS cloud phase is retrieved and classified into four categories; water, ice, mixed, and uncertain phase. Daily atmospheric data (MOD08, collocation 5) of MODIS gridded level-3 is collocated for the same validation period. MOD08 has the value of 1° pixel and is calculated by MOD06. MOD08 was used separately to analyze for average value of cloud retrieval information during the period of validation or the time-series analysis for a given grid.

3.4.3. Temporal and spatial collocation method

(1) CMDPS

we validated for each global area from Terra and Aqua satellite data. This validation is again divided into low and mid-latitudes. Low latitude was defined as the region below 30°and middle latitude was defined the region from above 30°to below 60°. In order to collocate the temporal and spatial collocation, the difference parts more than 2 pixels in 5x5 pixels of MODIS to validate in case of homogeneous region are excluded.

(2) Developer validation

For comparison of pixels, MODIS data inputted into the algorithm exactly corresponds to time and space.

3.4.4. Validation result analysis

(1) CMDPS validation CMDPS

The results analyzed for PC, PSS, HSS. It was improved for three algorithm modification and conditional validation. The results are shown in Table 4.

Table 4. Validation result of cloud phase

Reference	TIME		PC	PSS	HSS
MODIS (MOD06)	11/1~11/22	Global	0.626	0.556	0.445
		Low	0.703	0.690	0.511
		Mid	0.551	0.472	0.373
MODIS (MYD06)		Global	0.657	0.598	0.482
		Low	0.781	0.749	0.617
		Mid	0.536	0.509	0.346

For latitudinal validation, low latitudes have a higher accuracy than high latitudes. Also, validation results for Aqua satellites have higher accuracy than Terra.

(2) developer validation

(1) Scene analysis

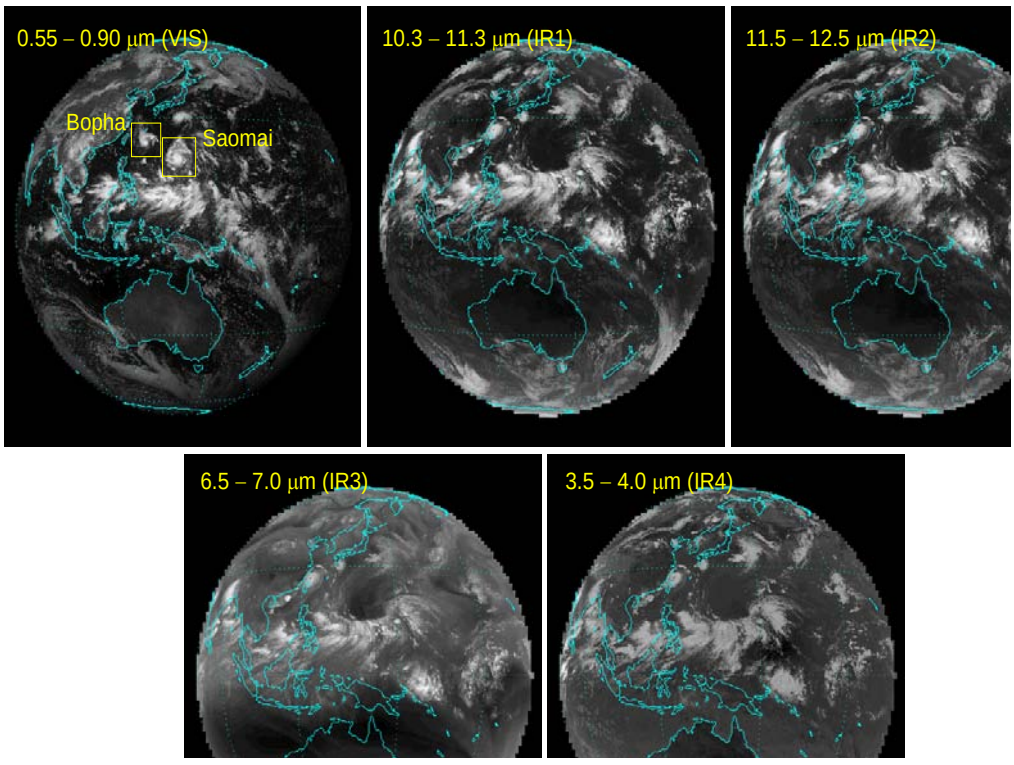

Fig. 7. JAMI/MTSAT-1R radiance imagery for the five spectral channels centered at 0.725㎛ (VIS), 10.8㎛

(IR1), 12.0㎛ (IR2), 6.75㎛ (IR3), and 3.75㎛ (IR4) for 0333 UTC August 7, 2006. Except for the VIS channel, the brighter color corresponds to a relatively low value in W m2 sr1 m1. The full-disk imagery covers East Asia, West Pacific, Australia, and a part of the Antarctic region (80.5S80.5N, 60.4E139.4W).

Fig. 7 is an example of JAMI radiance imagery at 0333 UTC on August 7, 2006. Clouds clearly show along the Intertropical convergence zone (ITCZ). Optically thick clouds scatter sunlight, and show brightly in the VIS image. Cloud above dark surfaces such as oceans are discriminated easily. A bright color In IR image corresponds relatively to low value. High altitude clouds show brightly because they emits a lower IR radiance from the top of the clouds. High clouds more than 400 hPa in IR3 images only show brightly. This is because water vapor absorption happens in middle to low level troposphere. Low clouds in the IR window channel such as IR1 or IR2 are clearly confirmed. IR4 radiance in general has a high value for small cloud particles, and water phase particles. When it considers the spectral properties of the 5 images discussed above, this time image is characterized by three great regions depending on inferred cloud properties.

(i) High clouds including clouds of Typhoon in the tropic western pacific region and optically thick clouds.

(ii) High clouds of Eastern pacific region and thin clouds

(iii) An extensive distributed region contains low and thin clouds, high and thick clouds over south-west ocean of Australia

(i) is inferred from high VIS, low IR1, low IR2 radiance, (ii) low VIS, low VIS, low IR2 radiance, (iii) extensively distributed low VIS, high IR1, high IR2 radiance and high VIS, low IR3 of spatial dendrite. We compared the three inferred properties of clouds and CMDPS algorithm product. At this step, all cloud information must be reviewed. Fig. 8 is a basic product (left) of cloud phase and final product (right). Overall, the difference between the two products is clear. The final product represents better the main properties of three clouds above mentioned for basic product. Final cloud phase has more water phase clouds and fewer uncertain clouds than the basic cloud phase.

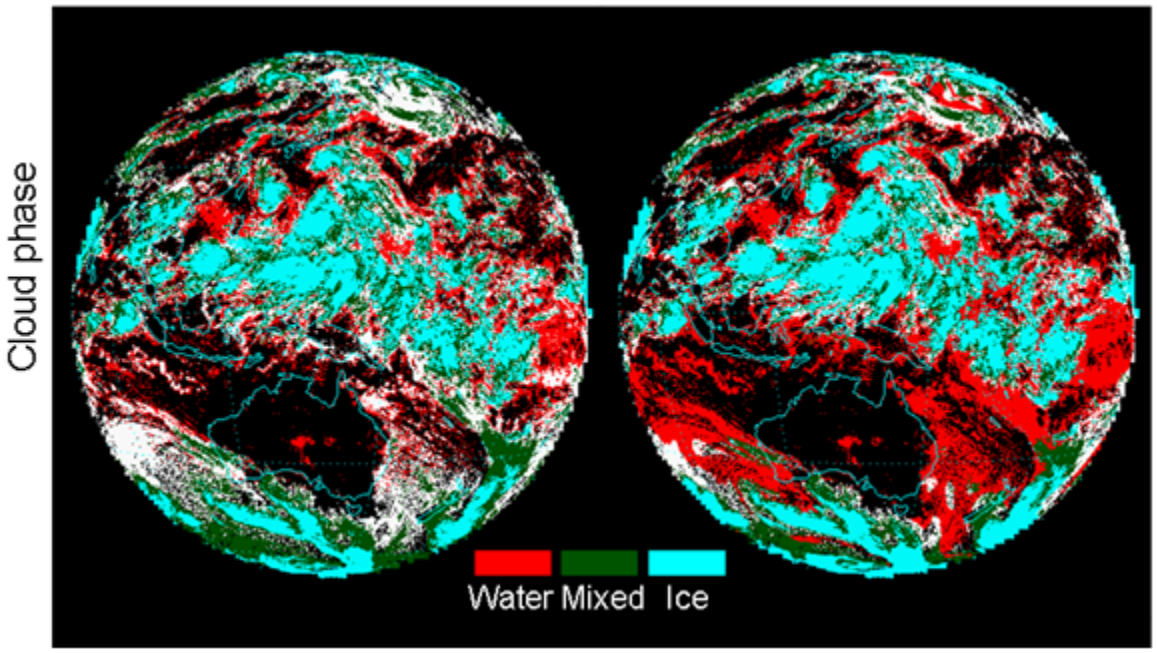

Fig. 8. Cloud phase derived by the CLA from the JAMI level-1b calibrated radiances shown in Fig. 7. Base products (left) are the results of conventional methods or without correction methods, and final products (right) from improved methods or with the correction methods developed in the present study.

(2) Climate data comparison

Table 3. shows the climate data of final, basic, and MODIS cloud phases. Retrieved cloud phase, MODIS cloud phase and climate data are very different. Water phase and ice phase clouds are found more in the final cloud phase than the basic cloud phase. The ratio is closer to the MODIS cloud phase. It means that additional water phase and ice phase through IR3 test is discriminated. If IR tests are not performed, many pixels will remain in the uncertain phase. This improved result does not seem to relate to the local time and region (Table 2).

. Mixed clouds in the final cloud phase are less than the basic cloud phase. Nevertheless, about 15% of pixels in the MODIS cloud phase remain uncertain.

The average in the polar region is below - 30℃ in all height and above 700 hPa minus is under 40℃ in above 700 hPa. We need to note the cloud phase of the polar region in particular. Our final cloud phase product shows 91.1% water phase and mixed phase. Interestingly, bispectral IR method from MODIS has a much smaller ratio. Water phase is 28.4%, and the uncertain phase is 17.4%. The supercooled water in middle cloud have higher temperature than minus 20 ℃ by Liou(2002) exists

such as ice particle.

최근 지상/항공 관측에 의한 보고에 의하면 영하 30 ℃ 미만의 온도에서도 구름 입자는 액체 수적을 가질 수 있다

According to reports by the recent surface/aviation measurements, Cloud particles under -30℃ can have liquid water. However, cloud phase in the polar region remains an issue to solve through more measurement (Shupe et al. 2006, Verlinde et al. 2007).

Table 5. Comparison of cloud phases from the JAMI/MTSAT-1R and the MODIS algorithm in August 2006. The numbers indicate the percentage of cloud phase (water/ice/mixed/uncertain) over the total cloud fraction. All results are calculated in the FOV of JAMI.

Domain		MTSAT CP		MODIS CP
		Final	Base	
Global	August	39.4/24.6/20.5/15.5	20.9/19.1/29.2/30.8	50.3/29.5/5.6/14.7
	Day	34.2/28.2/18.2/19.4	20.9/21.6/26.0/31.4	53.2/26.7/5.1/15.0
	Night	34.5/29.2/21.1/15.2	16.0/20.4/32.9/30.8	46.1/33.4/6.4/14.2
Northern Hemisphere		30.2/29.1/22.3/18.3	21.8/23.7/29.4/25.1	48.1/32.4/4.4/15.1
Southern Hemisphere		50.6/19.0/18.2/12.2	19.9/13.5/29.0/37.6	52.5/26.5/6.7/14.2
Polar		0.7/54.8/36.3/8.2	0.2/31.5/59.8/8.5	28.4/40.3/14.1/17.4
Midlatitude		28.9/19.6/29.8/21.7	8.8/12.9/40.4/37.9	52.7/23.8/6.8/16.7
Tropical		46.1/25.7/15.3/12.9	27.7/21.6/22.5/28.2	55.1/30.6/2.0/12.3

Products in mid-latitude and tropic region show the same difference. Our products have more ice phase and mixed phase, but MODIS has more water phase. Moreover, Mixed clouds in our product beside MODIS comprise more ratio. Clouds of this type seem to be identified with water phase in MODIS. Difference of this mixed phase use to discriminate mixed phase in MODIS at 8.5㎛ of the

main channel, but it is considered to show as this channel in algorithm do not exist. It is known that the MODIS CP algorithm does not detect high cirrus clouds consisting of ice particles (Menzel et al. 2006). In this algorithm, CP algorithm using the current IR still reconfirmed the uncertainty. Despite this, MODIS cloud phase and final product show a lot of difference, these are similar to the difference between conditions. Both nighttime cloud phases have a higher ratio of ice phase than daytime. This means to express diurnal variation of this cloud phase.. In addition, Both Northern Hemisphere cloud phases have more ice phase compared to the Southern Hemisphere. Because ITCZ locate in August Northern hemisphere. But this difference in basic cloud phase cannot see.

(3) Time-series comparison

Climate data comparison provides important information for validation, but it does not show the practical correspondence with MODIS product. This section analyzed time-series of product for nine areas of interest. It averaged hourly for 1° pixel in comparison with gridded MODIS MOD08 data, because it is retrieved in hourly 4km resolution. MODIS/Terra passes at 10:30 am for all regions. Therefore, hourly MTSAT data does not exactly coincide with MODIS data and time. This can only identify every hour variation and a similar diurnal variation. Fig. 9 represents the time series of the ratio of ice phase for total cloud amount in the basic cloud phase ((a) a gray line), final cloud phase ((b) a gray line), and MODIS cloud phase (thick line). Variation of the real cloud phase in this figure can know that it change quickly.

The effects of the basic IR3 test can know through comparison with cloud phase and final cloud phase, we can know that the effect depending on the region is different. In most regions, ice phase ratio is almost the same for MODIS data and its variation. When we used the IR3 test, it is more similar to the variation of MODIS in the final cloud phase.

However, the ratio of ice phase for the final cloud phase in the Antarctic region is higher than MODIS data (August 11-20, 25-31). When the period of validation consider in midwinter, ice phase cloud of high ratio is more realistic.

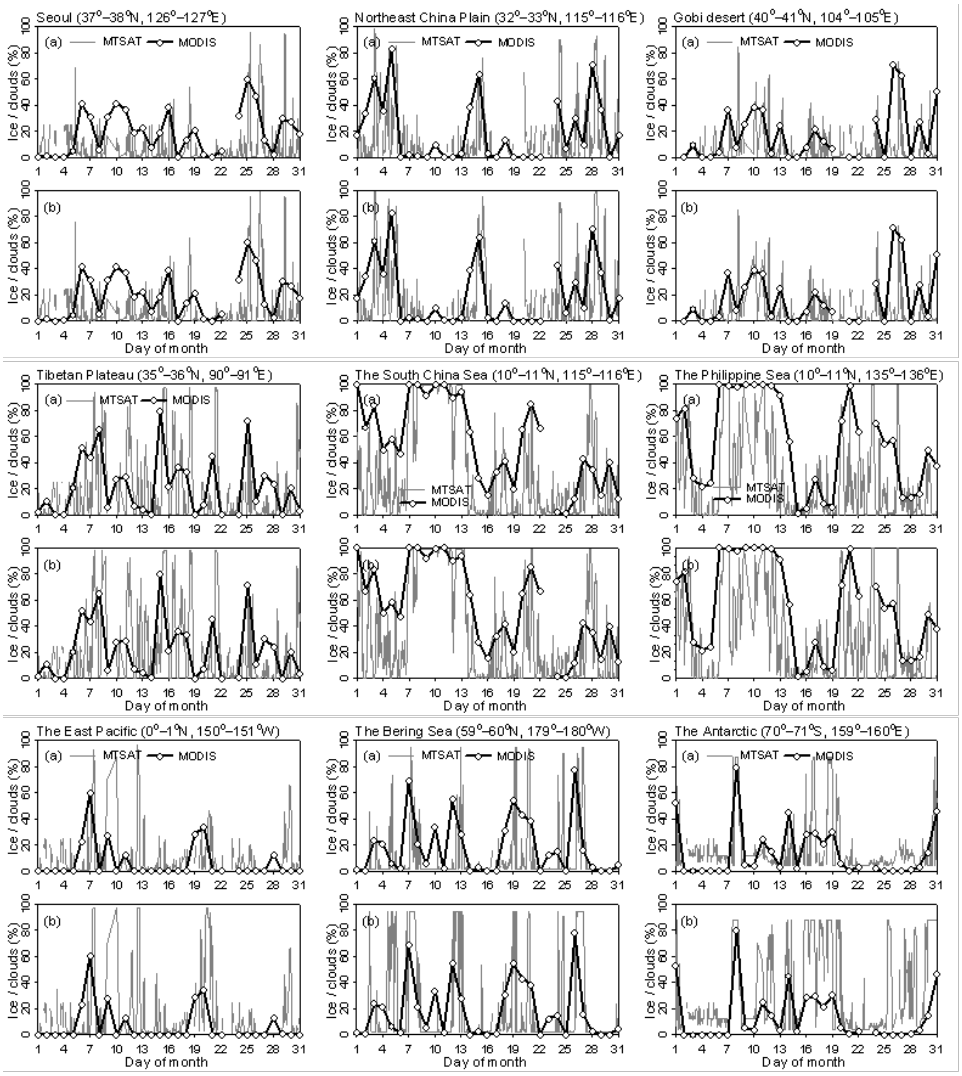

Fig. 9. Time series of the ratio of ice clouds to the total clouds at nine selected sites; base CP from IR1 and IR2 (a), and final CP from IR1, IR2, and IR3 (b).

(4) Pixel comparison

We arranged results in the table below compared with cloud phase to compare of exact pixels. The number in parenthesis is the result including the brightness temperature test of the 6.75㎛ channel. MODIS cloud phase and ice phase are more consistent.

Table 6. Comparison of cloud phase from the MODIS IR trispectral algorithm and from the algorithm for the COMS. The numbers (in parentheses) designate those from the algorithm from which BT6.7 is excluded (included).

COMS	MODIS					
	Clear	Water	Mixed	Ice	Uncertain	Total
Clear	13.0	0.0	0.0	0.0	0.0	13.0
Water	0.0	11.5 (19.7)	0.0	0.1 (0.3)	0.9 (4.1)	12.5 (24.1)
Mixed	0.0	2.3 (2.2)	7.1 (5.5)	21.2 (8.4)	5.8 (5.1)	36.4 (21.2)
Ice	0.0	0.0 (0.3)	0.0 (1.6)	15.6 (29.6)	0.0 (1.0)	15.6 (32.5)
Uncertain	0.0	13.8 (3.9)	0.0	3.9 (2.5)	4.9 (2.9)	22.6 (9.3)
Total	13.0	27.7	7.1	40.8	11.5	100.0

4. Interpretation method of retrieval result

The output data of cloud phase consist of water phase, ice phase, mixed phase, uncertain phase.

Table 7. Detailed Output data for the CP algorithm.

OUTPUT DATA								
Parameter	Mnemonic	Units	Min	Max	Prec	Acc	Res	To
Cloud phase	cloud_phase	-	-	-	-	-	pixel	CP

5. Problems and possibilities for improvement

6. References

Baum, B.A., Yang, P., Heymsfield, A.J., Platnick, S., King, M.D., Hu, Y.X. and Bedka, S.T., 2005, Bulk scattering properties for the remote sensing of ice clouds. Part II: Narrowband models. Journal of Applied Meteorology, 44, pp. 1896–1911.

Choi, Y.-S., Ho, C.-H. and Sui, C.-H., 2005, Different optical properties of high cloud in GMS and MODIS observations. Geophysical Research Letters, 32, L23823, doi:10.1029/2005GL024616.

Choi, Y.-S. and Ho., C.-H., 2006, Radiative effect of cirrus with different optical properties over the tropics in MODIS and CERES observations. Geophysical Research Letters, 33, L21811, doi:10.1029/2006GL027403.

Choi, Y.-S., Ho, C.-H., Ahn, M.-H. and Kim, Y.-M., 2007, An exploratory study of cloud remote sensing capabilities of the Communication, Ocean and Meteorological Satellite (COMS) Imagery. International Journal of Remote Sensing, 28, pp. 4715-4732.

Kim, J.-H., Ho, C.-H., Lee, M.-H., Jeong, J.-H. and Chen, D., 2006, Large increase in heavy rainfall associated with tropical cyclone landfalls in Korea after the late 1970s. Geophysical Research Letters, 33, L18706, doi:10.1029/2006GL027430.

King, M.D., Platnick, Hubanks, P.A., Arnold, G.T., Moody, E.G., Wind, G., and Wind, B., 2006, Collection 005 Change Summary for the MODIS Cloud Optical Property (06_OD) Algorithm. Available online at: modis-atmos.gsfc.nasa.gov/ C005_Changes/C005_CloudOpticalProperties_ver311.pdf.

Liou, K.N., 2002, An introduction to atmospheric radiation 2nd ed.. Academic Press, San Diego.

Menzel, W.P., Smith, W.L. and Stewart, T.R., 1983, Improved cloud motion wind vector and altitude assignment using VAS. Journal of Climate and Applied Meteorology, 22, pp. 377–384.

Menzel, W.P., Frey, R.A., Baum, B.A. and Zhang, H., 2006, Cloud top properties and cloud phase algorithm theoretical basis document, In MODIS Algorithm Theoretical Basis Document, NASA.

Platnick, S., King, M.D., Ackermann, S.A., Menzel, W.P., Baum, B.A., Riedi, J.C. and Frey, R.A., 2003, The MODIS cloud products: Algorithms and examples from Terra. IEEE Transactions on Geoscience and Remote Sensing, 41, pp. 456-473.

Rossow, W.B. and Garder, L.C., 1993a, Cloud detection using satellite measurements of infrared and visible radiances for ISCCP. Journal of Climate, 6, pp. 2341−2369.

____ and ____, 1993b, Validation of ISCCP cloud detections. Journal of Climate, 6, pp. 2370−2393.

____, Walker, A.W. and Garder, L.C., 1993, Comparison of ISCCP and other cloud amounts. Journal of Climate, 6, pp. 2394−2418.

____ and Schiffer, R.A., 1999, Advances in understanding clouds from ISCCP. Bulletin of the American Meteorological Society, 80, pp. 2261–2287.

Shupe, M.D., Matrosov, S.Y. and Uttal, T., 2006, Arctic mixed-phase cloud properties derived from surface-based sensors at SHEBA. Journal of the Atmospheric Sciences, 63, pp. 697711.

Strabala, K.I., Ackerman, S.A. and Menzel, W.P., 1994, Cloud properties inferred from 8–12-μm data. Journal of Applied Meteorology, 33, pp. 212–229.

Yang, P., Zhang, L., Hong, G., Nasiri, S.L., Baum, B.A., Huang, H.L., King, M.D. and Platnick, S., 2007,Differences between collection 4 and 5 MODIS ice cloud optical/microphysical products and their impact on radiative forcing simulations. IEEE Transactions on Geoscience and Remote Sensing, 45, pp.2886–2899.

Verlinde, J. and Coauthors, 2007, The mixed-phase arctic cloud experiment. Bulletin of the American Meteorological Society, 88, pp. 205221.